Electron Density Reconstruction and Optimum Beam Arrangement of Far-Infrared Interferometer in Heliotron J*)

Nan SHI, Shinsuke OHSHIMA, Kenji TANAKA[1)], Takashi MINAMI, Kazunobu NAGASAKI, Satoshi YAMAMOTO, Yoshiaki OHTANI[2)], Linge ZANG[2)], Tohru MIZUUCHI, Hiroyuki OKADA, Shinichiro KADO, Shinji KOBAYASHI, Shigeru KONOSHIMA, Naoki KENMOCHI[2)] and Fumimichi SANO

Institute of Advanced Energy, Kyoto University, Kyoto 611-0011, Japan
[1)]*National Institute for Fusion Science, Toki 509-5292, Japan*
[2)]*Graduate School of Energy Science, Kyoto University, Kyoto 611-0011, Japan*

(Received 20 November 2013 / Accepted 18 February 2014)

A multichannel far-infrared (FIR) laser interferometer is being developed for the helical-axis heliotron device Heliotron J with asymmetrical poloidal cross-section to study high-density plasma. Due to the shape of the cross-section, a new density reconstruction method based on the regularization technique was investigated for obtaining the electron density profile from the line-integrated density. For this purpose, the regularization parameter was optimized and determined by the generalized cross-validation (GCV) function and singular value decomposition (SVD). The reconstruction results show that the reconstructed profiles can be improved by carefully considering the beam position arrangement. The optimum beam arrangement is discussed in detail.

Keywords: electron density reconstruction, regularization, GCV, SVD, FIR interferometer, Heliotron J

DOI: 10.1585/pfr.9.3402043

1. Introduction

The electron density profile is critical for studying confinement and transportation in magnetically confined plasma. FIR laser interferometry, which provides the line-integrated density from the phase shift of a laser beam across the plasma, is widely used for routine diagnostics in thermonuclear fusion devices. In Heliotron J, which is a helical-axis heliotron device [1], a single-channel microwave interferometer and an amplitude modulation reflectometer have been used to measure the plasma electron density. Presently, for the study of high-density plasma, using advanced fuelling techniques, such as supersonic molecular beam injection (SMBI) or high-intensity gas puffing (HIGP), an FIR interferometer system is under development. The reconstruction of the density profile from line-integrated measurements in the highly asymmetrical poloidal cross-section of Heliotron J is complicated. Moreover, it is an ill-posed problem owing to the lack of available line-integrated data, caused by the available laser source power, beam divergence, device port limit, and so on. Therefore, a new reconstruction method, based on the regularization technique, was investigated, and it showed good compatibility and stability [2]. In this method, the generalized cross-validation (GCV) function [3, 4] is used in conjunction with singular value decomposition (SVD) to optimize the regularization parameter.

In this paper, the electron density reconstruction and optimum beam arrangement of the FIR interferometer in Heliotron J is discussed. The principle of the reconstruction method is introduced in section 2. The reconstruction results for different channel arrangements and magnetic configurations of Heliotron J are compared and discussed in section 3. Finally, the summary is given in section 4.

2. Reconstruction Method

In general, it can be assumed that the radial profile of density is discretized. In other words, the flux surface is separated into finite radial elements and labeled from core to edge as $j = 1, \ldots, n$. The local electron density is then assumed constant for each element. The jth element's local density in the radial region is represented by $n_{\mathrm{e}j}$ ($j = 1, 2, \ldots, n$). Thus, the ith element of the line integral density N_i measured by the interferometer is

$$N_i = \sum_{j=1,2,\ldots,n} L_{i,j} n_{\mathrm{e}j} \quad (i = 1, 2, \ldots, m), \tag{1}$$

where N_i contains elements of the channel number m. The matrix elements $L_{i,j}$ give the length of the ith optical path L_i in the flux zone j. Equation (1) can be expressed in matrix form as $\mathbf{N} = \mathbf{L} \times \mathbf{n}_{\mathrm{e}}$. In practice, m is less than n, and the direct inversion of L is impossible. Consequently, the interpolation of the measured integrated density is one of the methods to solve this problem, where N_i is interpo-

author's e-mail: nanshi@iae.kyoto-u.ac.jp
*) This article is based on the presentation at the 23rd International Toki Conference (ITC23).

lated from a size m to a size n array. Several studies have demonstrated the effectiveness of the technique [5, 6].

However, the technique is not applicable to noncircular plasmas, such as Heliotron J, because the accuracy of the interpolation and matrix inversion worsen for highly asymmetrical cross-sections. Therefore, the SVD–GCV method based on the regularization technique is introduced, and physically reasonable restrictions to avoid unrealistic solutions are imposed. The solution is derived by minimizing the following equation:

$$\frac{\mathbf{1}}{\mathbf{m}} \|\mathbf{N} - \mathbf{L} \times \mathbf{n}_\mathrm{e}\|^2 + \boldsymbol{\gamma} \|\mathbf{C}\mathbf{n}_\mathrm{e}\|^2 , \quad (2)$$

over the radial element of the flux surface. The Euclidean norm is denoted by $\|\cdot\|$. C is a kind of Tikhonov matrix and in this case Cn_e denotes the derivatives with respect to n_e for smoothing the solution. γ is a Lagrange multiplier, which determines the weighting between the goodness of fit and the smoothness requirement imposed on the solution. With increasing γ, the solution's dependability on $\|Cn_\mathrm{e}\|^2$ and the smoothness increases. While, with decreasing γ, the solution depends more on the goodness of fit.

The GCV function can be used to determine the optimum value of γ. The GCV is a transformed version of Allen's PRESS (prediction sum of squares) or ordinary cross validation, defined as the mean squared error between the predicted and observed data. The GCV estimate of γ is the minimization of $V(\gamma)$ given by

$$\mathbf{V}(\boldsymbol{\gamma}) = \frac{\mathbf{1}}{\mathbf{m}} \|(\mathbf{I} - \mathbf{A}(\boldsymbol{\gamma}))\mathbf{N}\|^2 \Big/ \left[\frac{\mathbf{1}}{\mathbf{m}} \mathbf{Tr}(\mathbf{I} - \mathbf{A}(\boldsymbol{\gamma}))\right]^2 , \quad (3)$$

where $\mathbf{A}(\boldsymbol{\gamma}) \equiv \mathbf{L}(\mathbf{L^T L} + \mathbf{m}\boldsymbol{\gamma}\mathbf{C^T C})^{-1}\mathbf{L^T}$ and I denotes the $m \times m$ unit matrix. Let SVD work on matrix $\mathbf{LC}^{-1}$ as $\mathbf{LC}^{-1} = \mathbf{U}\boldsymbol{\sigma}\mathbf{V^T}$, where $\boldsymbol{\sigma}$ is a $m \times n$ diagonal matrix whose entries are singular values. Then, substitute the decomposition results in Eqs. (2) and (3).

3. Design of the Interferometer based on the Reconstruction Study

3.1 Typical magnetic configurations of Heliotron J

By controlling the coil current of the five sets of external coils, the Heliotron J device can have wide range of magnetic configurations. To date, the study of configurations has focused on controlling the "bumpiness" effects on the plasma performance [7]. Different configurations have different magnetic surfaces; hence, density reconstruction is also influenced. Figure 1 shows the flux surfaces of three typical magnetic configurations (medium-, high-, and low-bumpiness configuration); clearly, the different configurations have different plasma shapes and sizes.

In Heliotron J, the electron density has finite values even at the last closed flux surface (LCFS); furthermore, low-density plasma exists in the ergodic region outside LCFS [6]. Thus, it is necessary to assume an isodensity surface outside the LCFS. The radial position for $n_\mathrm{e} \sim 0$ can be determined from Langmuir probe measurements, and accordingly, the zero density position is about 25 mm outside the LCFS [8]. The blue lines outside the LCFS are the flux surfaces expanded using the Variational Moments Equilibrium Code (VMEC) numerical equilibrium data [9].

3.2 Optimum measurement channel number and channel position effects

For reliable reconstruction of the density profile, sufficient measurement channels are necessary. However, two factors determine the number of channels: spatial limitation and performance of the hydrogen cyanide (HCN) laser source ($\lambda = 337\,\mu$m). The beam width of the laser limits the interval spacing between each pair of channels, while the total laser power restricts the number of measurement channels. The minimum channel spacing should be approximately 30 mm after considering the beam divergence of the laser. For determining the optimum channel number, four to seven channel cases are considered based on the assumed profiles.

If all channels are arranged in the half-part of the poloidal cross-section, the maximum channel number would be six owing to the spatial limitations discussed above. Because the magnetic configuration is up–down symmetric at the corner section of Heliotron J, one of the solutions to increase the channel number is to arrange the measurement channels to up and down parts, which reduces the effect of minimum spacing. For the seven-channel case, the arrangement is shown in Fig. 1 (c). In this study, the arrangement of the channels is also considered as a candidate of optimum arrangement.

Parameter d is the deviation between the reconstructed and assumed densities, and is expressed as

$$d = \sqrt{\left\langle \left(n_{\mathrm{e}i} - n_{\mathrm{e}i}^{assumed}\right)^2 \right\rangle}, \quad (4)$$

where $\langle\cdot\rangle$ denotes the average of all entries, and $n_{\mathrm{e}i}$ and $n_{\mathrm{e}i}^{assumed}$ are the ith reconstructed and assumed values, respectively.

Figure 2 shows the comparison of the reconstruction results using parameter d for each channel number case based on the same assumed hollow density profile. In this study, Four- to seven-channel cases are considered. Because of the strongly distorted flux surface, especially near the edge area, two types of channel position arrangements are chosen for each channel number case. One set of positions is arranging the channels with equal interval spacing, implying the channels are arranged at equal spacing from the core to the edge of the cross-section, as shown in Fig. 1 (a). The other set is arranging the channel position with unequal interval spacing, implying the channels are arranged in the noncircular region as shown in Fig. 1 (b). The red- and blue-colored symbols in Fig. 2

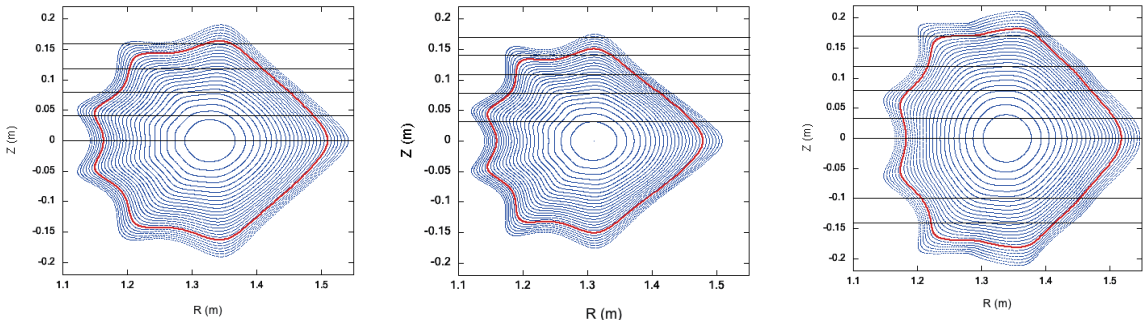

Fig. 1 Magnetic flux surfaces for (a) medium- (b) high-, and (c) low-bumpiness configurations. The blue lines inside the red rings show the flux surfaces inside the last closed flux surface (LCFS). The red lines show the LCFS and the blue lines outside the LCFS show the extrapolated surfaces. The black lines represent the examples of measurement channel arrangement of the interferometer system.

represent the equal and unequal interval spacing cases, respectively. Because different magnetic configurations have different plasma sizes, they affect the reconstructed density. Thus, as mentioned above, the reconstructed results for each set of positions' arrangement are calculated under three typical magnetic configurations (medium-, high-, and low-bumpiness configuration, shown in Fig. 1). For example, in the five-channel case, the red-colored symbols represent the results of arranging the channel positions with equal interval spacing (black lines in Fig. 1 (a)). The calculated magnetic flux surfaces are based on the medium-, high-, and low-bumpiness configuration, represented by the red circles, red triangles, and red squares, respectively. Based on the three types of typical magnetic flux surfaces, the blue symbols are for the unequal interval spacing (black lines in Fig. 1 (b)). Other channel number cases use the same descriptions as in Fig. 2.

In the four- and five-channel cases with equal spacing, the reconstruction results are unstable and with greater uncertainties owing to the limits of the beam channels, which fails to follow the changes in the density profile. However, the results for the cases with unequal spacing are better than the cases with equal spacing, especially for the four- and five-channel cases. Parameter d of the five-channel cases is as good as that in the six- and seven-channel cases. Actually, for each channel number case, several sets of channel positions with unequal interval spacing are tested. Based on the calculations, it is calculated that approximately $Z = 0.1$ (Z is the ordinate in Fig. 1) is a sensitive position. For $Z > 0.1$, the distortion of the flux surface becomes stronger and causes the reconstruction to fail. The reconstructed density can be obtained with good accuracy only if at least three channels are arranged outside $Z = 0.1$.

The five-channel case with unequal spacing is concluded to be the optimum channel arrangement. In strongly shaped plasma, if the measurement channels are limited, the channel arrangement will have to be considered carefully. The required channel number can be reduced if the channel position is properly arranged by considering the cross-section shape.

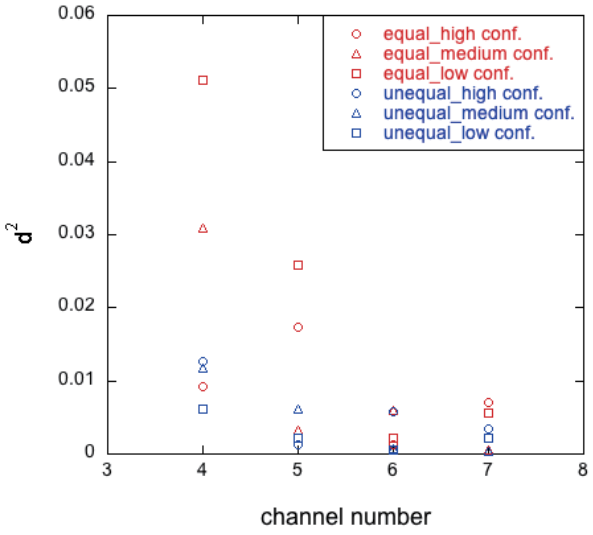

Fig. 2 Comparison of evaluated errors for four, five, six, and seven channels. The red symbols show the results of channel arrangement at equal interval spacing. The blue symbols show the results at unequal interval spacing.

For the three magnetic configurations, the reconstruction results for the five-channel case with equal and unequal interval spacing are shown in Fig. 3. Figures 3 (a and b) and 3 (c and d) show the results for equal interval spacing and unequal interval spacing, respectively. The peaked and hollow profiles, observed in Heliotron J, are chosen as the assumed profiles.

Figure 3 shows that for peaked profiles, the reconstruction results are in agreement with the assumed ones for equal and unequal spacing. For the hollow profile case, the reconstruction results for the unequal spacing arrangement show better stability than the equal spacing arrangement.

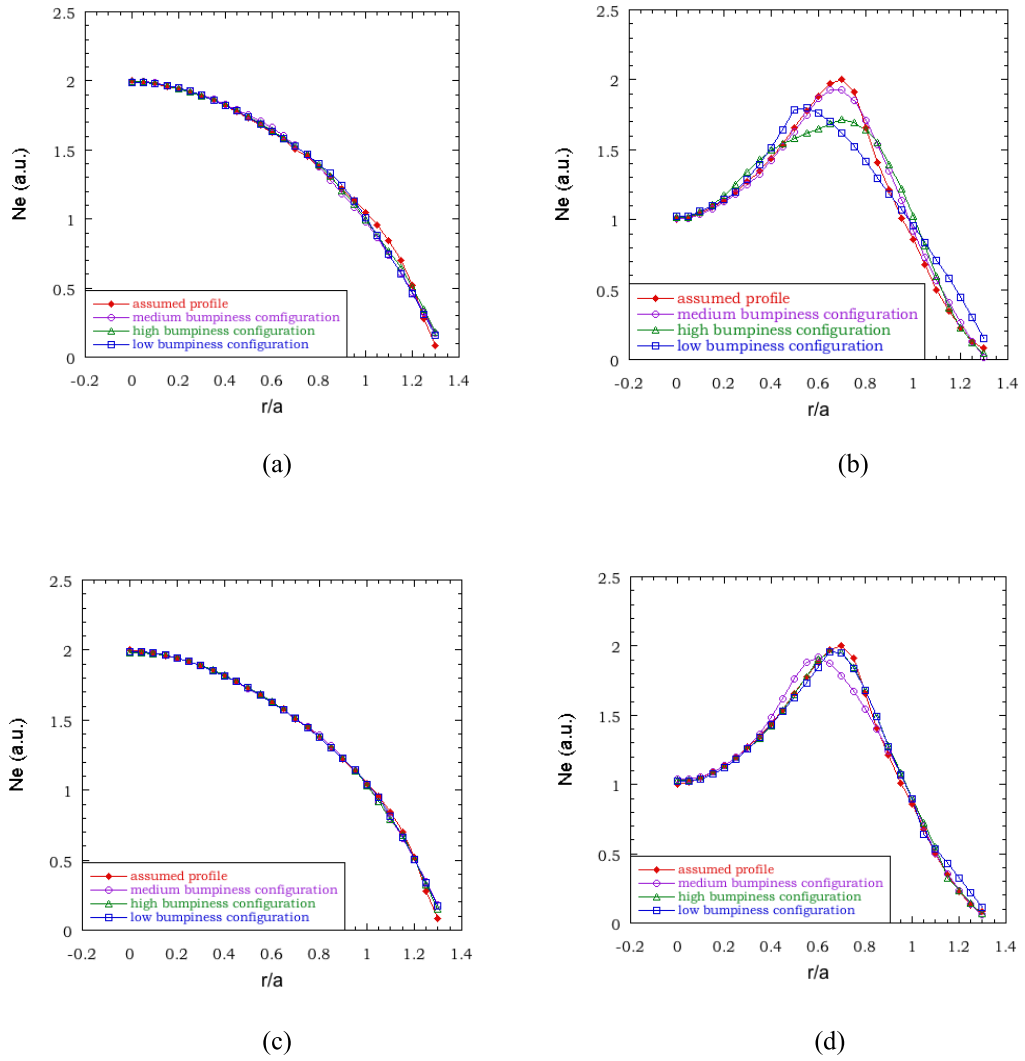

Fig. 3 Comparison of reconstruction results for the five-channel case with equal and unequal spacing arrangement. The channel position for equal spacing in (a) and (b) is represented by black lines in Fig. 1 (a); the channel position of unequal spacing in (c) and (d) is represented by the black lines in Fig. 1 (b). The red dotted line represents the assumed profile. The purple dotted line represents the results for medium-bumpiness magnetic configuration, shown in Fig. 1 (a). The green dotted line represents the results for high-bumpiness magnetic configuration, shown in Fig. 1 (b). The blue dotted line represents the results for low-bumpiness magnetic configuration, shown in Fig. 1 (c).

4. Summary

The optimum beam arrangement of an FIR interferometer has been obtained according to the reconstructed density profiles using the SVD–GCV method. The method is based on the regularization technique; the GCV function is used to optimize the regularization parameter in conjunction with SVD. As shown in Fig. 1 (b), the reconstruction results show that in Heliotron J, five measurement channels with unequal interval spacing arrangement may give acceptable density profiles. We conclude that in strongly shaped plasmas, properly arranged channel positions are critical for reconstructing the density profiles. If the channel position is properly chosen, the measurement channel number will decrease, and the reconstructed density profile can be obtained with good accuracy from the reduced channels.

[1] T. Obiki, T. Mizuuchi, K. Nagasaki, H. Okada *et al.*, Nucl. Fusion **41**, 833 (2001).
[2] N. Shi, S. Ohshima, K. Tanaka, T. Minami *et al.*, submitted to Rev. Sci. Instrum.
[3] G.H. Golub, M. Heath and G. Wahba, Technometrics **21**, 215 (1979).
[4] N. Iwama, H. Yoshida, H. Takimoto, Y. Shen *et al.*, Appl. Phys. Lett. **54**, 502 (1989).
[5] Hyeon K. Park, Plasma Phys. Control. Fusion **31**, 2035 (1989).
[6] K. Tanaka, K. Kawahata, T. Tokuzawa, S. Okajima *et al.*, Plasma Fusion Res. **3**, 050 (2008).
[7] T. Mizuuchi, F. Sano, K. Kondo *et al.*, Fusion Sci. Technol. **50**, 1 (2006).
[8] T. Mizuuchi, K. Murai, S. Watanabe, S. Yamamoto *et al.*, J. Nucl. Mater. **390-391**, 428 (2009).
[9] S.P. Hirshman and W.I. van Rjj, Comput. Phys. Commun. **43**, 143 (1986).